TISSUE ENGINEERING: Part A
Volume 21, Numbers 1 and 2, 2015
© Mary Ann Liebert, Inc.
DOI: 10.1089/ten.tea.2013.0403

Hyaluronidase-Loaded PLGA Microparticles as a New Strategy for the Treatment of Pulmonary Fibrosis

Claudia da Silva Bitencourt, PhD,[1,5] Guilherme Martins Gelfuso, PhD,[2] Priscilla Aparecida Tartari Pereira, PhD,[1] Patrícia Aparecida de Assis, PhD,[1] Cristiane Tefé-Silva, PhD,[3] Simone Gusmão Ramos, PhD,[3] Eliane Candiani Arantes, PhD,[4] and Lúcia Helena Faccioli, PhD[1]

The aim of this work was to develop an innovative tool for the treatment of pulmonary fibrosis based on our previous findings, which demonstrated that intranasally administered soluble bovine hyaluronidase (HYAL) increases the numbers of mesenchymal (MSC)-like cells in the bronchoalveolar fluid (BALF) and thus reduces the bleomycin-induced fibrosis. To this end, we developed poly(D,L-lactide-co-glycolide) (PLGA) microparticles (MPs) loaded with HYAL (HYAL-MP) to preserve the enzyme's biological activity and to facilitate its delivery to the lung. Nonloaded MPs (Control-MPs) and HYAL-MPs were prepared using the emulsion and solvent evaporation methods and thoroughly characterized. The HYAL-MPs and Control-MPs exhibited an average diameter of 4.3 ± 2.1 and 4.4 ± 1.5 μm, respectively. The encapsulation efficiency of the HYAL-MPs was 68%, and encapsulation led to a reduced release rate. Additionally, the HYAL-MPs were efficiently phagocytosed by J-774.1 cells. Compared with the soluble HYAL, the HYAL-MPs increased the proportion of MSC-like cells in the BALF of C57BL6 mice 96 h after treatment. The efficacy of the HYAL-MPs was also tested in C57BL6 mice that were previously exposed to 4 U/kg of bleomycin to induce lung fibrosis. The results demonstrated that the HYAL-MPs reduced neutrophil recruitment after bleomycin treatment more effectively than did the soluble HYAL, whereas the Control-MPs did not exhibit any effect. The HYAL-MPs also reduced the bleomycin-induced fibrosis more efficiently, and 134% of the collagen deposition in the lung compared with the soluble HYAL and the Control-MPs. In summary, our data indicate that HYAL-MPs are an effective delivery system that could feasibly be used in the treatment of pulmonary fibrosis.

Introduction

Although idiopathic pulmonary fibrosis (IPF) is the most common interstitial pneumonia, the cause of IPF remains unknown. The disease may be triggered by epithelial injury and apoptosis, unpaired re-epithelization, or aberrant wound healing, but its pathogenesis is poorly understood.[1] Transforming growth factor (TGF), fibroblasts, and myofibroblasts mainly contribute to excessive extracellular matrix and collagen deposition, which disrupts the lung architecture.[2,3] The prevalence of IPF is 13 to 20 cases per 100,000 individuals, and the incidence is increasing with a survival time of 3 to 5 years after diagnosis.[1,4] Despite the morbidity of this disease, few therapies have successfully improved the survival and quality of life of IPF patients, which has resulted in a continued search for new therapies.[5]

Hyaluronidase (HYAL) has been widely used in therapy due to its ability to spread drugs in certain tissues, increase vascular permeability, and reduce the viscosity of biological fluids.[6,7] In mammals, HYAL is a component of urine, plasma, and seminal fluid,[8] whereas, in poisonous animals, the enzyme is a nontoxic component of venoms that is important to the envenomation process.[8] In contrast, in bacteria, HYAL is considered a virulence factor.[9] HYAL regulates the hyaluronic acid levels and the remodeling of the extracellular matrix.[8,10]

We recently demonstrated that IPF therapy using soluble bovine HYAL decreased bleomycin-induced fibrosis, which indicates a new use for this enzyme.[11] We also established that a single intranasal dose of soluble HYAL increased mesenchymal (MSC)-like cells and ameliorated pulmonary fibrosis, specifically through the reduction of collagen

[1]Departamento de Análises Clínicas, Toxicológicas e Bromatológicas, Faculdade de Ciências Farmacêuticas de Ribeirão Preto, Universidade de São Paulo,- Ribeirão Preto, Brazil.
[2]Departamento de Ciências Farmacêuticas, Faculdade de Ciências da Saúde, Universidade de Brasília, Brasília, Brazil.
[3]Departamento de Patologia, Faculdade de Medicina de Ribeirão Preto, Universidade de São Paulo, Ribeirão Preto, Brazil.
[4]Departamento de Física e Química, Faculdade de Ciências Farmacêuticas de Ribeirão Preto, Universidade de São Paulo, Ribeirão Preto, Brazil.
[5]Centro Universitário das Faculdades Associadas de Ensino (FAE) São João da Boa Vista, Brazil.

deposition and TGF-β production.[11] However, HYAL is easily degraded,[12] which renders it difficult to use for the treatment of fibrosis.

Poly(D,L-lactide-co-glycolide) (PLGA)-based microparticles (MPs) have been extensively used as carriers for the controlled delivery of therapeutics, such as proteins, peptides, genes, growth factors, and lipids.[13–15] Additionally, certain pharmaceutical and biomedical products composed of PLGA have already been approved by the U.S. Food and Drug Administration (FDA) for use in humans (e.g., Resomer® and Lactel®).[16]

Proteins have been successfully entrapped in MPs and used as vaccines or therapies. We recently developed MPs containing cell-free antigens from *Histoplasma capsulatum* that have great potential as a vaccine because these MPs efficiently activate mononuclear cells.[17,18] It is known that microencapsulation protects proteins, lipids, and drugs from degradation and enhances their potency and efficacy.[13–15] The entrapment of proteins and other products in delivery systems specifically increases the potency of vaccines and therapies by preserving the stability and biological activity of the encapsulated agents.

The delivery of proteins with therapeutic potential through the inhalation route is a challenge and considered the most promising noninvasive route. The major problems associated with this delivery route are the clearance of the delivery system by alveolar macrophages and the mucociliary apparatus and the correct delivery to the lung airways.[19,20] To avoid these problems, optimal aerodynamic properties must be achieved to ensure that the MPs reach the deep lungs when inhaled.[20] The efficient drug delivery to the lungs is driven by the particle size, shape, deposition, dissolution, and clearance metabolism of the lung drug delivery system.[21]

In this study, we developed an innovative strategy to treat pulmonary fibrosis by encapsulating HYAL in PLGA MPs, which would both preserve the activity of HYAL and increase the potency of the enzyme's effects. Our results demonstrate that the encapsulated enzyme was more powerful than soluble HYAL in decreasing lung inflammation and fibrosis.

Materials and Methods

Animals

C57BL6 mice (20–25 g) were obtained from the facilities of the Faculdade de Ciências Farmacêuticas de Ribeirão Preto, Universidade de São Paulo. The experiments were conducted according to the guidelines of the Animal Care Committee of the Universidade de São Paulo (Protocol No. 07.1.782.53.8).

MP preparation

The MPs loaded with HYAL were prepared using the double emulsion and solvent evaporation technique. Briefly, 120 mg of polymer (PLGA 50:50) was dissolved in 10 mL of methylene dichloride, and this mixture was emulsified with 0.2 mL of an inner aqueous phase containing bovine HYAL (2.75 mg) using an Ultra-Turrax T-25 homogenizer (IKA Labortechnik). The emulsion was then poured into 40 mL of PVA solution in water (3%, w/v). This final double emulsion was stirred at 600 rpm for 4 h using an RW-20 homogenizer (IKA Labortechnik) to induce solvent evaporation. The MPs were then collected, washed for 6 min at 23,600 *g* with sterile water, and freeze-dried by lyophilization during 24 h for storage at −20°C. The control MPs, which did not contain HYAL, were prepared using the same method. All of the MPs were prepared under sterile conditions.

MP characterization

The diameters of the HYAL-MPs and Control-MPs were determined using an LS 13 320 Laser Diffraction Particle Size Analyzer (Beckman Coulter). The zeta potentials were characterized using a Zetasizer Nano (Malvern Instruments). In both cases, 1 mg of MPs was dispersed in 0.4 mL of distilled water and analyzed at 25°C. The morphologies of the dried MPs were assessed by scanning electron microscopy using a Zeiss Scanning Microscope (Evo 50). Before being taken to the microscope, 3 mg of the liophylized MPs were sprinkled on a platform and coated with gold.

HYAL encapsulation efficiency. The encapsulation efficiency (EE%) of the HYAL-MPs was assessed by dissolving 10 mg of the MPs in 0.6 mL of acetonitrile under agitation to disrupt them. The acetonitrile was then dried using a Concentrator plus (Eppendorf®) and 1 mL of water was added to dissolve HYAL and precipitate the polymer PLGA. The mixture was filtered using a 0.22 μm membrane and the HYAL concentration were indirectly quantified using a Coomassie protein assay kit. The EE% was calculated based on the following formula:

$$\mathrm{EE}\% = (\text{total amount of protein detected in MPs} / \text{total amount of protein theoretically associated with MPs}) \times 100$$

HYAL release rate. The HYAL release rate was assessed using a modified Franz-type diffusion cell (Microette; Hanson Research) and a cellulose acetate membrane with a pore size of 0.45 μm (Fisher). Three milligrams of HYAL-MPs were suspended in 300 μL of saline buffer and placed on the membrane in the donor compartment. Samples (1 mL) were collected at 0.5, 1, 1.5, 2, 3, 4, 6, 9, 12, 24, and 48 h, and the diffusion of soluble HYAL was analyzed using a Coomassie protein assay kit®. The same experiment was performed using nonloaded bovine HYAL. The enzymatic activity of the HYAL released from the MPs was also turbidimetrically assessed following the protocol described by Bordon *et al.*[22]

Endotoxin measurements. The possible presence of lipopolysaccharide in the MPs was assessed using a *Limulus amebocyte* lysate test following the manufacturer's instructions.

Cellular uptake of MPs

J-774 cells were cultured (2×10^5 cells/well) in 24-well plates with a 13-mm circular cover slip in each well. After 1 h, the medium was removed, and 1 mL of a 1 mg/mL dispersion of HYAL-MPs or Control-MPs in RPMI-1640 was added. After 4 h, the noningested MPs were gently washed away. The cover slips were stained with Panoptic. In

some sets of experiments, the uptake was inhibited using 5 μg/mL/well of cytochalasin D. The MP uptake was assessed by counting 200 cells that did or did not ingest the MPs and the total number of engulfed MPs. The phagocytic index (PI) was calculated as follows: PI = number of engulfed MPs × number of cells containing at least one MP/total number of cells counted.

Experimental design and treatments

In one set of experiments, mice were intranasally (i.n.) inoculated with 16 U of soluble HYAL or 2 mg of HYAL-MPs. The controls received phosphate-buffered saline (PBS) or 2 mg of Control-MPs. The amount of 2 mg of MP is equivalent to 16 U of HYAL as determined by % encapsulation. All of the preparations were administered in a volume of 20 μL of sterile PBS that was slowly dropped into the nasal cavity of the mice. Ninety-six hours after the treatment, the animals were euthanized. In another set of experiments, bleomycin sulfate was administered intratracheally (4 U/kg in 0.9% NaCl in a total volume of 100 μL).[11,23] After 8 days of bleomycin treatment, the animals were treated i.n. with 16 U of soluble HYAL, 2 mg of HYAL-MPs, 2 mg of Control-MPs, or PBS. Ninety-six hours after treatment, the animals were euthanized. The cells from the bronchoalveolar space were collected, stained, and counted as previously described.[11]

Immunophenotyping of cells. The expression levels of CD34, CD73, SCA-1 (Ly-6AE), and CD90.1 on the surface of the cells from the bronchoalveolar fluid (BALF) were determined through immunostaining and flow cytometry, as previously described.[11]

Cytokine measurement. Interleukin (IL)-13, tumor necrosis factor (TNF)-α, TGF-β, monocyte chemotactic protein-1 (MCP-1), and keratinocyte chemoattractant (KC) were assessed in the lung homogenates of the C57BL6 mice by ELISA according to the manufacturer's instructions (BD Biosciences). The sensitivity of the assays was > 10 pg/mL.

Collagen assay. The soluble collagen in the supernatants of the homogenates of the lung parenchyma was quantified as previously described.[11,24]

Analysis of gene expression by real-time polymerase chain reaction. The total RNA was isolated from the lung tissue using the TRIzol reagent according to the manufacturer's instructions. The reverse transcription of 1 μg of RNA was performed using a high-capacity cDNA archive kit. Subsequently, the mRNA expression of *Tgfb*1 and *Tgfbr*1 was evaluated by real-time polymerase chain reaction (PCR) using the TaqMan method, and all of the samples were processed in duplicate. The probes used for the amplification were synthesized by an Assays-on-Demand system (Applied Biosystems) based on the following GenBank sequences: *Tgfb*1 (NM_011577.1) and *Tgfbr*1 (NM_009370.2). The *Hprt* (NM_008722.2) probe was included as an endogenous control. The PCR analysis used the StepOnePlus™ Real-Time PCR System (Applied Biosystems), and the $2^{-\Delta\Delta CT}$ method was used to evaluate the PCR data and the relative gene expression in a particular sample as follows: relative amount of target = $2^{-\Delta\Delta CT}$.

Histopathological analysis. The lungs of the mice were fixed in formalin 10%. After 48 h the specimens were processed routinely and stained with hematoxylin and eosin (H&E) and Picro Sirius Red. The surface density of the collagen fibers in the lung was determined by assessing optical density. More specifically, images were captured using a video camera (Leica Microsystems) coupled to a microscope DMR (Leica Microsystems GmbH) and a computer. These images were processed using Leica QWin software (Leica Microsystems Image Solutions). After enhancing the contrast to a point at which the fibers were easily identifiable as red bands, the thresholds for the collagen fibers were established for each slide. Ten randomly chosen, no coincident fields were measured at a magnification of 200× across a frame area of 0.28 mm^2. The resultant values were expressed as a percentage of the area.[24,25]

Statistical analysis

The data were expressed as the mean ± standard error of the mean. The statistical variations were determined using Student's *t*-test or analysis of variance and the Newman–Keuls post test. The results were analyzed using the GraphPad Prism 5.0 software, and differences with $p < 0.05$ were considered statistically significant.

Results

First, we encapsulated HYAL in PLGA MPs. The HYAL-MPs exhibited a mean hydrodynamic diameter characterized using laser diffraction of 4.3 ± 2.1 μm with a monomodal distribution. Similarly, the Control-MPs, which did not encapsulate HYAL, presented an average diameter of 4.4 ± 1.5 μm (Table 1). The zeta potential of the Control-MPs was −21.7 ± 4.4 mV, and this surface charge was modified to −2.6 ± 7.8 mV by the incorporation of HYAL. This neutralization of the particles' surface charge indicates that there may be an interaction between the polymer and HYAL, which suggests a successful drug encapsulation. HYAL seems to modify the negative electric load of the polymer.

Figure 1 depicts photomicrographs of the Control-MPs (Fig. 1B, C) and the HYAL-MPs (Fig. 1D, E). All of the particles were reasonably spherical in shape, and the images confirm the size range of the particles, as determined by laser diffraction. The encapsulation efficiency of the HYAL-MPs was 68% ± 5%, which was interesting considering the method of double emulsification. Figure 1A also shows the HYAL release profile for the MPs compared with the dissolution/diffusion of nonencapsulated HYAL. The MPs reduced the release rate of the enzyme in a progressive, zero-order manner ($r = 0.99$). HYAL was specifically released from the MPs with a calculated flux of 0.88%/h. It is important to mention that our *in vitro* analysis was

Table 1. Mean Diameter (μm) and Zeta Potential (mV) of HYAL-MPs in Comparison with Control-MPs

	Mean diameter (μm)	*Zeta potential (mV)*
HYAL-MPs	4.3 ± 2.1	−2.6 ± 7.8
Control-MPs	4.4 ± 1.5	−21.7 ± 4.4

HYAL, hyaluronidase; MPs, microparticles.

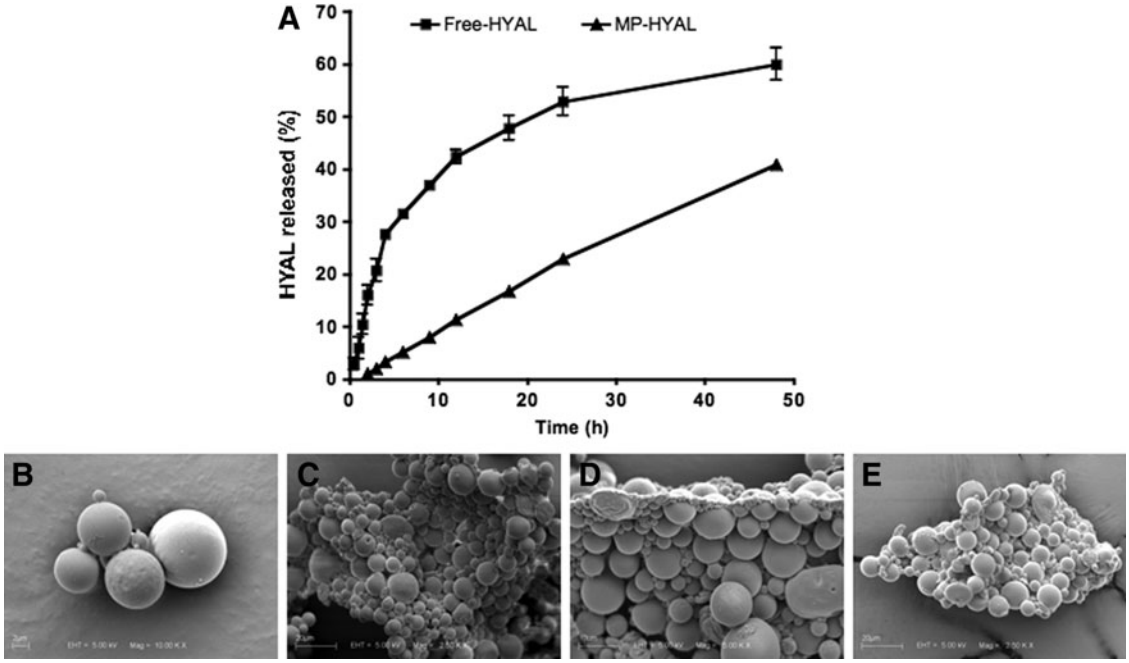

FIG. 1. Characterization of HYAL-MP. **(A)** The release profile of HYAL from the HYAL-MPs compared with the diffusion of nonloaded HYAL (Free-HYAL). The data are presented as the mean ± SD of three replicates. Scanning electron microscopy images of the **(B, C)** HYAL-MPs and **(D, E)** Control-MPs. The MPs shown are representative of the different batches. HYAL, hyaluronidase; MPs, microparticles.

performed during 48 h; however, at this time point there was an incomplete release of HYAL because a plateau was not observed in the HYAL-MP curve. The HYAL activity remained higher than 80% in all of the samples, which shows that the encapsulation process did not significantly alter the activity. The endotoxin levels detected in the MPs were lower than 0.1 EU/kg, which indicates that the MPs were adequate for therapeutic use based on the criteria of the European Pharmacopoeia (5 EU/kg/h is the safety level required for endovenous administration). Taken together, the data show that the delivery system developed in this work is appropriate for the intranasal administration of HYAL and could be used therapeutically.

Our next *in vitro* studies were designed to determine whether the HYAL-MPs would be recognized and efficiently phagocytosed by macrophages. To achieve this objective, we used J-774 cells, which are of a murine macrophage lineage. Figure 2 shows that the HYAL-MPs were properly recognized and phagocytosed by macrophages. Moreover, the macrophages internalized the HYAL-MPs more frequently than the Control-MPs (Fig. 2A, B). Figure 2C shows that the addition of cytochalasin D to the culture inhibited the uptake, which demonstrates that both preparations entered the macrophage via phagocytosis.

We then determined whether the effects of the HYAL-MPs on the healthy lung microenvironment were similar to the effects of soluble HYAL. Mice were intranasally inoculated with a single dose of 16 U of HYAL, 2 mg of HYAL-MPs, or 2 mg of Control-MPs. The BALF cells were recovered 96 h after treatment. The soluble HYAL induced a late and nearly exclusive increase in mononuclear cells in the BALF, and the HYAL-MPs presented the same pattern of cell recruitment (Fig. 3B). This finding shows that the biological effect of HYAL was preserved after encapsulation. As expected, the Control-MPs did not augment the mononuclear cell numbers in the lung 96 h after inoculation (Fig. 3B).

Using flow cytometry, we also examined whether the cells in the BALF of the mice treated with soluble HYAL, HYAL-MPs, or Control-MPs were MSC-like 96 h after the inoculation. The cells were incubated with antibodies against CD34, CD73, SCA-1 (Ly-6AE), and CD90.1, which is a panel of antigens used to characterize MSC-like cells. We observed important differences between the cells induced by the three stimuli (Fig. 3D). When the inoculations with the soluble HYAL and HYAL-MPs were compared, the overlaid histograms indicated marked disparities in the expression of the cell surface markers. More specifically, the expression of CD73, CD90.1, and SCA-1 on the surface of the BALF cells after HYAL-MP inoculation (green histogram) was higher than the expression following soluble HYAL treatment (blue histogram). Additionally, by comparing the expression of CD73, CD90.1, and SCA-1 after HYAL-MP administration, we noticed that the CD90.1 surface expression on the BALF cells was higher than the CD73 and SCA-1 expression, and different results were obtained after soluble HYAL administration. To investigate possible inflammation in the lung parenchyma, the tissue obtained from mice inoculated with PBS, soluble HYAL, HYAL-MPs, or Control-MPs was stained with H&E. As observed in Figure 3C, inoculation with the Control-MPs or HYAL-MPs did not change the cells in the lung parenchyma compared with PBS inoculation.

Given that the cells in the BALF of mice inoculated with the HYAL-MPs or soluble HYAL were phenotypically similar to MSCs, we further analyzed the potential to

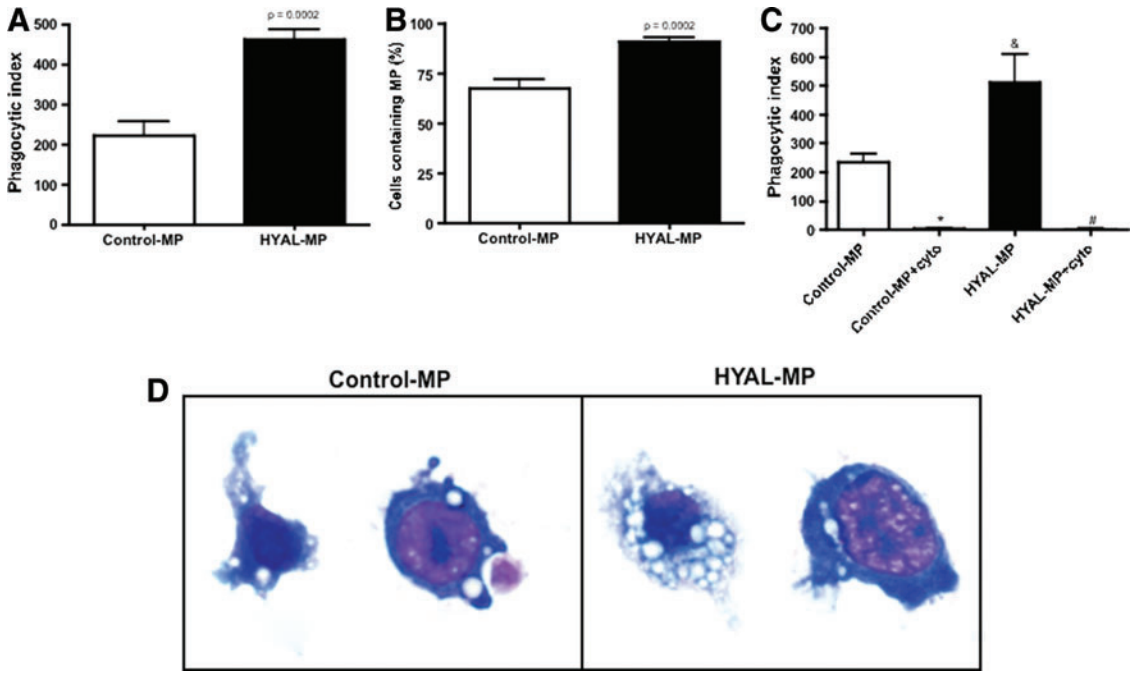

FIG. 2. MPs are recognized by phagocytic cells by mechanisms dependent on cytoskeleton. **(A)** The uptake of Control-MPs and HYAL-MPs by J-774 cells after 4 h of incubation. Briefly, J-774 cells were plated (2×10^5 cells/well) and after 1 h, 1 mg/mL HYAL-MPs or Control-MPs were added. After 4 h, cells were stained. The phagocytic index was then calculated as described in the Materials and Methods section. The values represent the mean ± SEM from one representative result of three independent experiments ($n = 6$; $p = 0.0002$ compared with the Control-MPs, as determined using Student's *t*-test). **(B)** The percentages of J-774 cells that engulfed at least one MP. The values denote the mean ± SEM from one representative result of three independent experiments ($n = 6$; $p = 0.0002$ compared with the Control-MPs, as determined using Student's *t*-test). **(C)** Uptake of the Control-MPs and HYAL-MPs by J-774 cells was inhibited by cytochalasin D, a cytoskeleton inhibitor. Briefly, J-774 cells were plated (2×10^5 cells/well). After 1 h, 5 μg/mL/well of cytochalasin D was added, and, after 30 min, 1 mg/mL HYAL-MPs or Control-MPs in RPMI-1640 were added. After 4 h, cells were stained with Panoptic. The phagocytic index was then calculated. The values express the mean ± SEM from one representative result of two independent experiments ($n = 6$; $^{\&}p < 0.001$ and $^{*}p < 0.01$ compared with the Control-MPs, $^{\#}p < 0.001$ compared with the HYAL-MPs. One-way ANOVA was used. **(D)** Representative photomicrographs of J-774 cells that phagocytized Control-MPs or HYAL-MPs. The cells on glass slides were stained with Panoptic and photographed using light microscope. Magnification: 100×/1.25 oil. ANOVA, analysis of variance; SEM, standard error of the mean. Color images available online at www.liebertpub.com/tea

diminish bleomycin-induced pulmonary fibrosis. The mice were exposed to bleomycin on day 0, and, 8 days after bleomycin exposure, the mice were treated intranasally with a single dose of sterile PBS, soluble HYAL, HYAL-MPs, or Control-MPs. The BALF was recovered 96 h after the treatment, and the BALF cells were enumerated to confirm the presence of inflammatory exsudate. The period after the treatments exhibited an increase in the proportion of MSC-like cells in the BALF after inoculation with the postsoluble HYAL or HYAL-MPs. As expected, the soluble HYAL caused an insignificant reduction in neutrophil recruitment following bleomycin exposure. In contrast, the HYAL-MPs significantly reduced the number of these cells (Fig. 4A), and this was followed by a significant decrease in mononuclear cells (Fig. 4B) compared with the PBS or soluble HYAL treatments. The total soluble collagen assayed using Sircol was decreased in mice treated with either soluble HYAL or HYAL-MPs compared with the PBS-treated animals (Fig. 4C).

The cytokines involved in the progression of lung fibrosis were also evaluated after bleomycin exposure and soluble HYAL, HYAL-MPs, or Control-MPs treatment. The MCP-1, IL-13, TNF-α, and KC levels were not significantly altered by these treatments compared with mice inoculated with bleomycin and treated with sterile PBS (Fig. 5A–D). However, a significant decrease in the TGF-β concentration was observed in the lung homogenates after the soluble HYAL or HYAL-MPs treatment compared with the PBS treatment (Fig. 6A). In addition, we observed significant reduction in the mRNA expression of Tgfb1 and Tgfbr1 (Fig. 6B, C).

Finally, we analyzed the morphology of the lung and collagen deposition after the inoculation of bleomycin and either HYAL, HYAL-MPs, Control-MPs, or PBS treatment. Histopathological analysis of the lungs of the mice inoculated with bleomycin and treated with sterile PBS revealed subpleural and parenchymal foci of inflammation and fibrosis (Fig. 7). In contrast, the soluble HYAL treatment reduced the bleomycin-induced fibrosis and collagen deposition. Unexpectedly, the treatment with the HYAL-MPs led to a more marked reduction in the lung inflammation and collagen deposition compared with the treatment with the soluble HYAL. As mentioned before, the total soluble collagen was also decreased in mice treated with either soluble HYAL or HYAL-MPs. Additionally, the collagen deposition in the tissue was measured using Picrosirius Red, and a

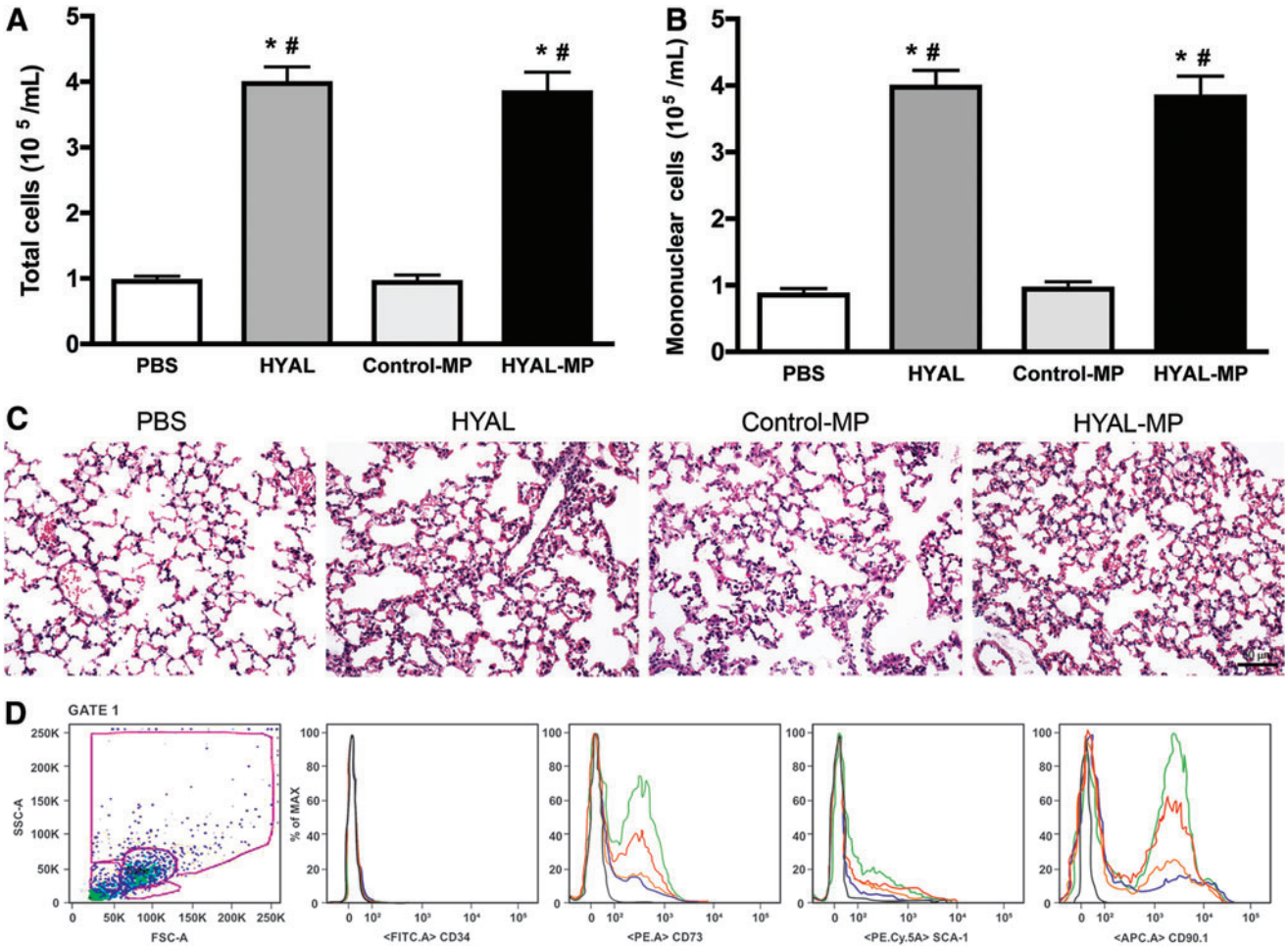

FIG. 3. Soluble HYAL and HYAL-MPs induce an increase in leukocyte numbers in bronchoalveolar space. Total leukocyte **(A)** and mononuclear cell **(B)** present in bronchoalveolar fluid (BALF) recovered 96 h after intranasal inoculation of phosphate-buffered saline (PBS), 16 U of bovine testicular HYAL, 2 mg of Control-MPs, or 2 mg of HYAL-MPs. The values represent the mean ± SEM from one representative result of three independent experiments ($n = 5$; $^{*}p < 0.001$ compared with PBS and $^{\#}p < 0.001$ compared with the Control-MPs; the significance levels were determined by ANOVA). **(C)** Photomicrographs of representative healthy lung sections obtained from C57BL/6 mice 96 h after intranasal inoculation of 16 U HYAL, 2 mg of Control-MPs, or 2 mg of HYAL-MPs. The tissues were stained with hematoxylin and eosin. Original magnification: 200×, Scale bar: 50 μm **(D)** HYAL and HYAL-MPs induce an increase cells with an MSC-like phenotype. Gate 1 is a representative image depicting the forward- and side-scatter dot plots of the cells in the BALF. The histograms overlays were performed using the gated population (gate 1): the *dotted black histogram* = isotype; the *red histogram* = PBS; the *blue histogram* = soluble HYAL; the green histogram = HYAL-MPs; and the *orange histogram* = Control-MPs. This figure depicts a representative analysis from three independent experiments. Color images available online at www.liebertpub.com/tea

greater decrease was observed after the HYAL-MPs treatment compared with the soluble HYAL treatment (Fig. 4D). Taken together, these data show that both the soluble HYAL and the HYAL-MPs significantly reduced the bleomycin-induced pulmonary fibrosis. Our results also demonstrate that the soluble HYAL and the HYAL-MPs reduced the histopathological manifestation of lung fibrosis by decreasing the neutrophil numbers, the collagen content, and the TGF-β production.

The H&E staining revealed subpleural and parenchymal foci of inflammation and fibrosis in the mice inoculated with bleomycin, and these foci were more reduced after the HYAL-MP treatment compared with the soluble HYAL treatment (Fig. 7A). The same pattern of decreased fibrosis was observed in the lungs stained with Picrosirius Red, which labels collagen deposition (Fig. 7B). Additionally, as mentioned previously, the measured collagen deposition in the tissue showed that the HYAL-MPs were more effective than the soluble HYAL in decreasing this deposition because the HYAL-MP treatment resulted in a 134% decrease in the amount of deposited collagen compared with that obtained with soluble HYAL. Additionally, HYAL-MP was fivefold more effective in the reduction of the neutrophil numbers compared with soluble HYAL and achieved an 8% higher reduction of TGF-β compared with soluble HYAL.

Discussion

These studies of the effects of HYAL-MP lung administration revealed potentially important new findings. First, we

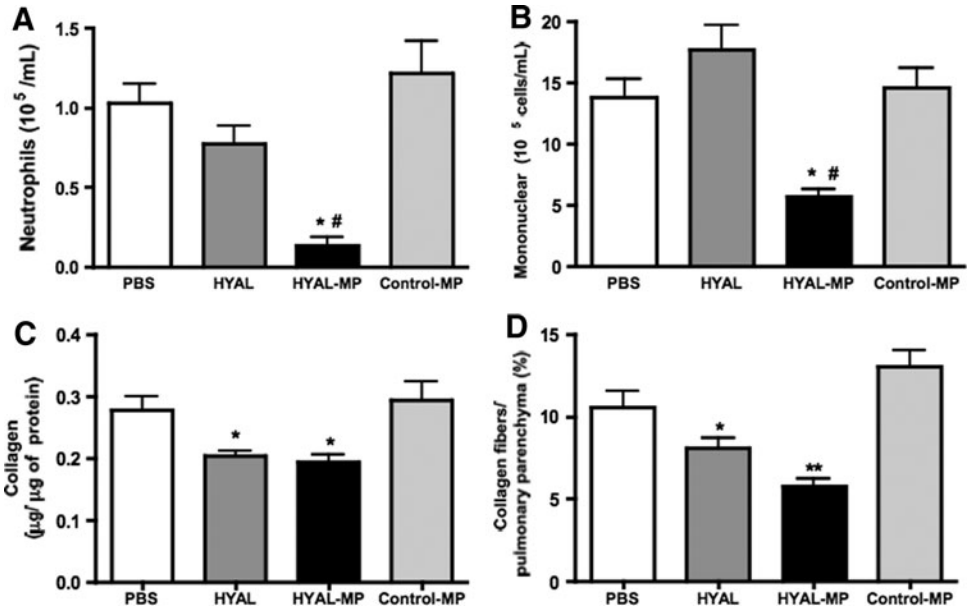

FIG. 4. HYAL-MP treatment reduces alveolar leukocyte numbers numbers and collagen deposition in bleomycin-induced fibrosis. Eight days after bleomycin inoculation (4 U/kg/0.1 mL 0.9% NaCl) to lungs of C57BL/6 mice, the animals were intranasally treated with PBS, 16 U of soluble HYAL, 2 mg of Control-MPs, or 2 mg of HYAL-MPs. Bronchoalveolar cells were recovered 96 h after treatments, and **(A)** neutrophils and **(B)** mononuclear-cells in bleomycin-inoculated lungs were counted. The values represent the mean ± SEM ($n = 5$; $^{*}p < 0.05$ compared with PBS and $^{\#}p < 0.05$ compared with soluble HYAL; the significance levels were determined by ANOVA). **(C)** The acid-soluble collagen in the supernatant of the lung homogenates was assayed using Sircol. The values represent the mean ± SEM ($n = 4$; $^{*}p < 0.05$, $^{**}p < 0.01$ compared with PBS, as determined by ANOVA). **(D)** The area occupied by the collagen fibers was determined by Picrosirius Red morphometric analysis and digital densitometry. The data were expressed as a percentage of the total area of the field. The values represent the mean ± SEM ($n = 4$; $^{*}p < 0.05$, $^{**}p < 0.01$ compared with PBS, as determined by ANOVA).

demonstrated that HYAL-MP constitutes a feasible system to delivery HYAL. Second, HYAL-MP recruited cells that had phenotypic features of MSC-like cells. Third, we demonstrated that treatment with HYAL-MP reduced more efficiently than soluble HYAL the bleomycin-induced fibrotic response in the lung parenchyma.

Our delivery system was designed to achieve lung environment. Size is particularly important in the development of a system for pulmonary delivery because a particle must have a diameter of less than 10.0 µm to reach the lower airways.[26,27] The pulmonary delivery of proteins requires that the particles for delivery be in the aerodynamic size

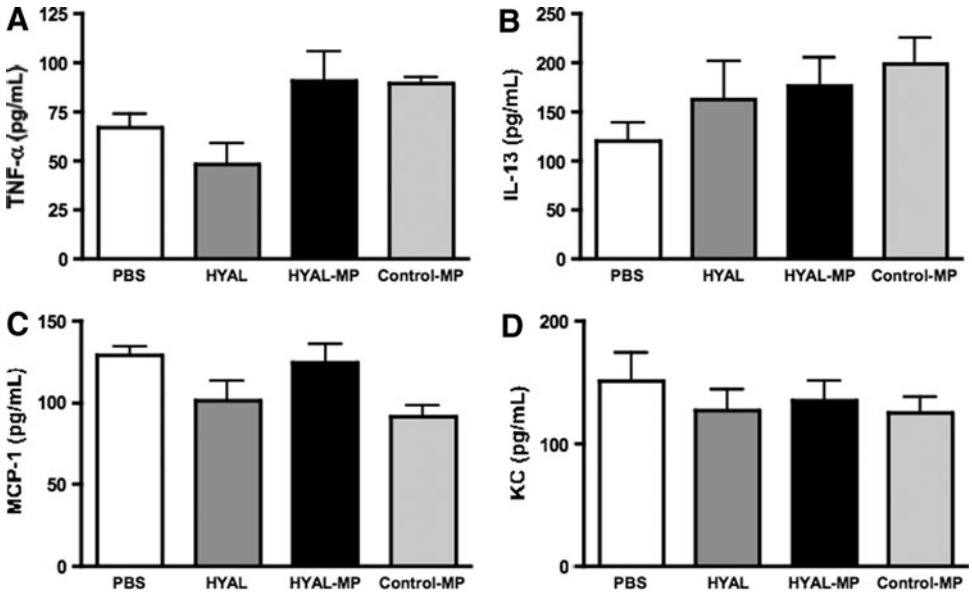

FIG. 5. Soluble HYAL, HYAL-MPs, and Control-MPs did not modify cytokines production in lung of bleomycin-inoculated mice. **(A)** Tumor necrosis factor (TNF)-α, **(B)** Interleukin (IL)-13, **(C)** Monocyte chemotactic protein-1 (MCP-1), and **(D)** Keratinocyte chemoattractant (KC) were assayed by ELISA. The values represent the mean ± SEM ($n = 5$).

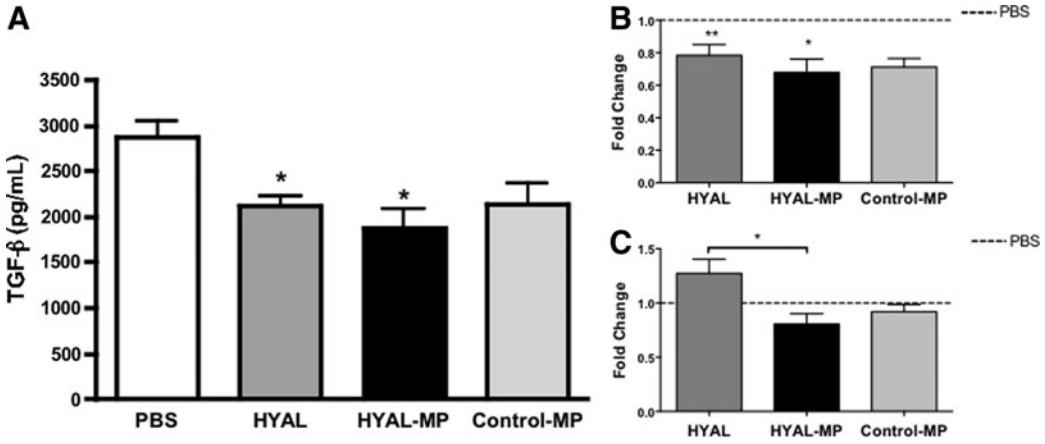

FIG. 6. Transforming growth factor-β (TGF-β) and mRNA in lung parenchyma of bleomycin-inoculated mice intranasally treated with soluble HYAL, HYAL-MPs, and Control-MPs. **(A)** TGF-β was assayed by ELISA. The values represent the mean ± SEM ($n = 5$; $*p < 0.005$ compared with PBS, as determined by ANOVA). The mRNA expression of **(B)** *Tgfb1* and **(C)** *TgfbRI* was evaluated by real-time polymerase chain reaction. The *Hprt* probe was included as an endogenous control. The gene expression values were presented as the fold change ($2^{-\Delta\Delta Ct}$) using the relative expression in the animals treated with PBS as a reference (*dotted line*). The samples were processed in duplicate, and the data were analyzed using ANOVA ($n = 5$; $*p < 0.05$, $**p < 0.01$ compared with PBS).

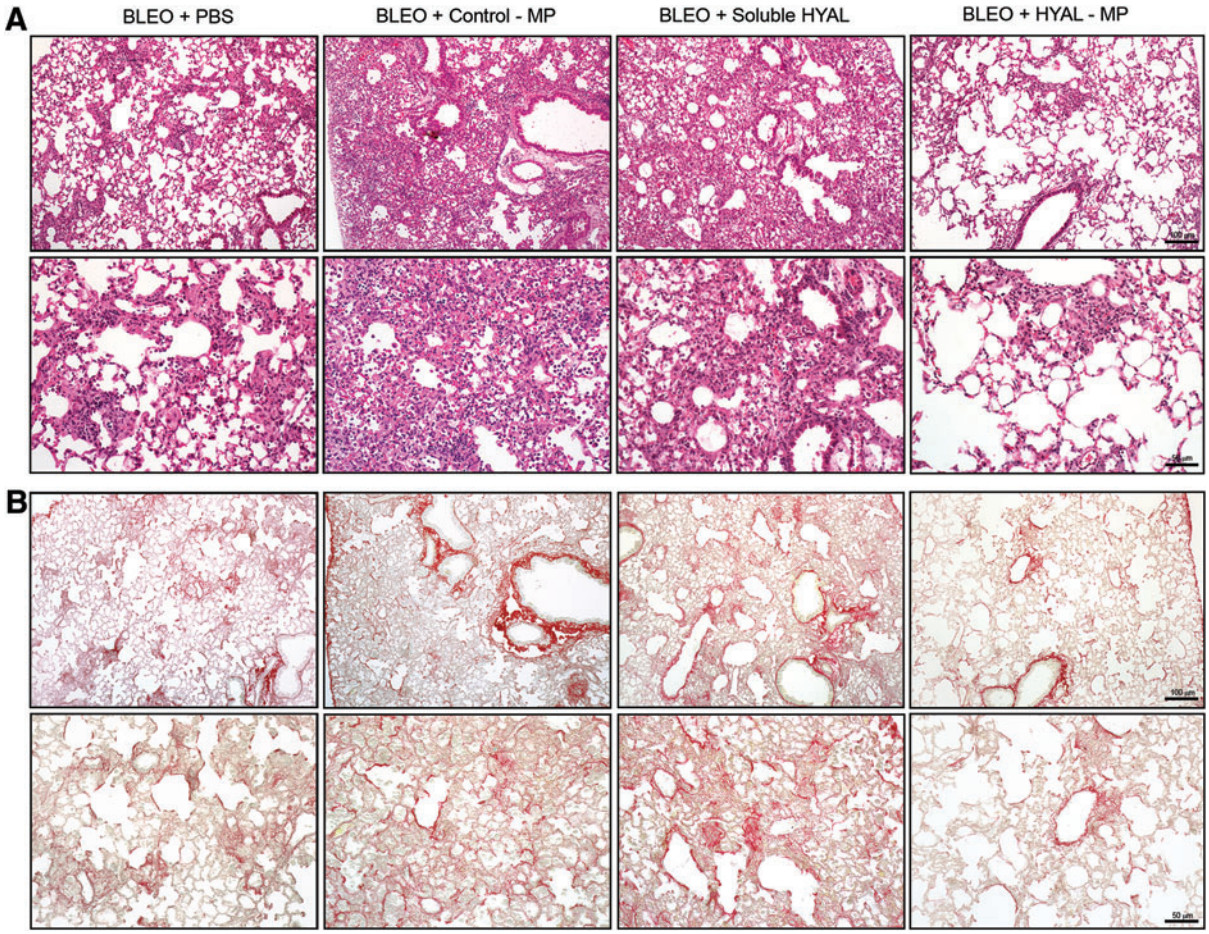

FIG. 7. HYAL-MPs reduce lung inflammation and collagen deposition in a bleomycin-induced lung fibrosis. Photomicrographs of representative lung sections obtained from mice inoculated with bleomycin and intranasally (i.n.) treated with PBS, 16 U of soluble HYAL, 2 mg of Control-MPs, or 2 mg of HYAL-MPs. **(A)** The tissues were stained with hematoxylin and eosin to investigate the accumulation of inflammatory cells (original magnification: 100× and 200×, scale bars: 50 and 100 μm, respectively). **(B)** The tissues were stained with Picrosirius Red to determine the collagen content (original magnification: 100× and 200×, scale bars: 50 and 100 μm, respectively). Color images available online at www.liebertpub.com/tea

range of 1 to 5 μm to achieve deep lung deposition correlated with a good clinical response for local treatment.[19,21] MPs bigger than 5 μm are retained in the oropharyngeal region through inertial collision, whereas particles between 1 and 5 μm are deposited in the bronchioles and alveoli through gravitational sedimentation.[19] This reduced size of our MPs might therefore facilitate the development of a pulmonary delivery system in powder form, which is simpler, inexpensive, and more stable. Our results suggest that HYAL can donate positive charge to the polymer surface; however, this alteration does not compromise the uptake of the particles by macrophages. Previous studies have shown that the diffusion of hydrophilic compounds from the inner to the outer aqueous phase reduces the drug encapsulation.[18] In our study, the larger size of the therapeutic agent (HYAL: ≈55 kDa) may have reduced the agent's diffusion through the organic phase of the emulsion during the MP preparation, thereby improving the HYAL encapsulation. The preservation of enzymatic activity is also important because the effect of soluble HYAL is partially dependent on its activity.[11] We observed that the encapsulation process did not alter the enzymatic activity. Our data showed that HYAL-MP constituted an adequate delivery system, preserving both activity and release of HYAL.

Next, we analyzed whether HYAL-MP could be recognized and entrapped by macrophages. Our result confirms that MPs smaller than 10 μm in diameter are efficiently phagocytosed by macrophages.[19,28,29] Also, using cytochalasin D to the culture to bind to actin filaments and block polymerization and the elongation of actin we demonstrated that MP entered the macrophage via phagocytosis.

Next, we verified whether HYAL-MP could induce the same unusual cell migration to the lung observed in a work using soluble HYAL.[11] Here, we also demonstrated the unusual profile of cellular migration induced by HYAL and that MP-HYAL recruits mesenchymal-like cells to the lung. Cell recruitment is one of the components of the inflammatory process that is regulated by soluble mediators released from resident cells and later from inflammatory cells. Typically, neutrophils are the first cells recruited to an inflammatory site, and these are followed by mononuclear cells.[28] However, both soluble and encapsulated HYAL did not induce neutrophil recruitment to the bronchoalveolar space and lung parenchyma. Instead, the cells recruited to the lung by either stimulus were nearly exclusively mononuclear cells, in accordance with our previous results.[11] It is important to mention that these proteins are the most common surface markers used to characterize MSCs. According to the Mesenchymal and Tissue Stem Cell Committee of the International Society for Cellular Therapy (ISCT), the positive expression of CD90.1 and CD73 is considered the minimal criterion defining MSCs.[29,30] Notably, in a previous work,[11] we fully characterized the cells recruited to the bronchoalveolar space after soluble HYAL inoculation as MSC-like because these cells exhibited surface marker expression similar to the expression on MSCs obtained from cord blood.[31] Based on our data, we suggest that the cells that accumulated in the BALF following HYAL-MP treatment were also MSC-like.

Consistent with our previous results,[11] the soluble HYAL caused an insignificant reduction in neutrophil recruitment following bleomycin exposure. The results presented here show that the HYAL-MPs had the same ability to recruit MSC-like cells to the bronchoalveolar space as soluble HYAL, which is consistent with our previously published data.[11] Additionally, the biological activity of the HYAL-MPs was preserved in the healthy lung. It is known that neutrophils play an important role in the pathogenesis of IPF and are increased in the BALF of IPF patients.[32] Therefore, the decrease in neutrophil numbers observed here may lessen the bleomycin-induced fibrosis.

The cytokines involved in the progression of fibrosis[2] were also evaluated after bleomycin exposure and we did not observe alterations in the cytokines analyzed except TGF-β. A significant decrease in the TGF-β concentration was observed after HYAL-MPs treatment. Consistent with that, we also observed a decrease in mRNA expression of *Tgfb*1 in mice treated with both HYAL and HYAL-MP, however, the gene expression of the major TGF-β receptor TBRI was reduced in mice treated with HYAL-MP compared with soluble HYAL treatment.

The TGF-β pathway is regulated in a positive feedback loop, in which TGF-β is required to increase the level of its own mRNA and the mRNA of the TGF-β receptor.[33,34] Thus, the decreased gene expression and production of TGF-β can be the responsible for the decrease expression of its receptor TBRI. In a bleomycin-treatment model using the soluble TGF-β receptor as a therapeutic strategy, it was demonstrated that this molecule possesses antifibrotic potential *in vivo* and thus constitutes an effective treatment for fibrosis.[35] Additionally, TGF-β has been observed to play a role in the development of fibrosis, possibly as the main switch that triggers disease progression.[36] This cytokine, which is produced by alveolar epithelial cells, also drives the differentiation of fibroblasts into myofibroblasts that secrete excessive amounts of collagen.[3] A therapeutic approach that decreases TGF-β levels could therefore ameliorate fibrosis. In light of these previous findings, our intranasally delivered HYAL-MPs constitute a feasible strategy for the treatment of lung fibrosis.

As described previously,[1,11] a histopathological analysis of the lungs of the mice inoculated with bleomycin and treated with sterile PBS revealed subpleural and parenchymal foci of inflammation and fibrosis. Our data demonstrated that both HYAL and HYAL-MP are able to reduce fibrosis. However, although the effects of the soluble HYAL and HYAL-MPs appear comparable, there were important differences between the treatments that indicate that the HYAL-MPs are clearly more effective than the soluble HYAL. Pulmonary fibrosis and other conditions have been investigated as potential targets for MSC therapy because MSCs can differentiate into diverse lung cells.[37] A review of our current understanding of the role of stem and progenitor cells in lung repair encourages cell-based and novel bioengineering approaches as therapeutic strategies to repair and remodel the lung after injury.[30] Cell-based therapy has typically been an important means of ameliorating fibrosis, as in a study using umbilical cord MSCs that diminished bleomycin-induced fibrosis.[38] The disadvantages of this therapy are related to the fact that classical stem cell therapy can increase the risk of allergic reactions and bacterial and viral infections.[39,40] Moreover, the high numbers of cells that must be transplanted are difficult to obtain, and there are no standardized methods for collecting these cells.[41] In this study, using MPs loaded with HYAL, we present an

innovative, alternative approach for the treatment of fibrosis. In this therapy, the encapsulated enzyme appears to reduce fibrosis. Based on our data, we suggest that this reduction in the lung fibrosis by HYAL occurs due to three distinct events: (i) fractionation of the lung hyaluronan, which generates different fragments that regulate inflammation,[10] (ii) decreased TGF-β production and collagen deposition, and (iii) increased numbers of MSC-like cells in the lung.[11]

In summary, we have demonstrated that both soluble HYAL and HYAL-MPs decrease lung fibrosis and that HYAL-MPs are more efficient than soluble HYAL and thus constitute a novel, alternative strategy for the amelioration of pulmonary fibrosis.

Conclusions

Encapsulation in PLGA, preserve the biological activity of HYAL and the HYAL-MPS are appropriate for intranasal administration route since they exhibit an adequate size, zeta potential, and release rate. The effects of the HYAL-MPs were similar to the effects of the soluble HYAL: both recruit mononuclear cells with MSC-like phenotypes into the healthy lung. Moreover, in lungs with bleomycin-induced fibrosis, the HYAL-MPs were more effective than the soluble HYAL in decreasing inflammation, TGF-β production, and collagen deposition. We propose that HYAL-MP administration is a novel strategy for the treatment of pulmonary fibrosis.

Acknowledgments

The authors would like to acknowledge J.O.D. Ciampo, F.R. Moraes, K.C.F. Bordon, and E.M. Floriano for the technical assistance. These studies were funded by the Fundação de Amparo a Pesquisa do Estado de São Paulo (FAPESP) and the Conselho Nacional de Desenvolvimento Científico e Tecnológico (CNPq).

Disclosure Statement

No competing financial interests exist.

References

1. Mouratis, M.A., and Aidinis, V. Modeling pulmonary fibrosis with bleomycin. Curr Opin Pulm Med **17,** 355, 2011.
2. Hardie, W.D., Glasser, S.W., and Hagood, J.S. Emerging concepts in the pathogenesis of lung fibrosis. Am J Pathol **175,** 3, 2009.
3. King, T.E., Jr., Pardo, A., and Selman, M. Idiopathic pulmonary fibrosis. Lancet **378,** 1949, 2011.
4. Raghu, G., Weycker, D., Edelsberg, J., Bradford, W.Z., and Oster, G. Incidence and prevalence of idiopathic pulmonary fibrosis. Am J Respir Crit Care Med **174,** 810, 2006.
5. O'Connell, O.J., Kennedy, M.P., and Henry, M.T. Idiopathic pulmonary fibrosis: treatment update. Adv Ther **28,** 986, 2011.
6. Menzel, E.J., and Farr, C. Hyaluronidase and its substrate hyaluronan: biochemistry, biological activities and therapeutic uses. Cancer Lett **131,** 3, 1998.
7. Dunn, A.L., Heavner, J.E., Racz, G., and Day, M. Hyaluronidase: a review of approved formulations, indications and off-label use in chronic pain management. Expert Opin Biol Ther **10,** 127, 2010.
8. Kemparaju, K., and Girish, K.S. Snake venom hyaluronidase: a therapeutic target. Cell Biochem Funct **24,** 7, 2006.
9. Hynes, W.L., Dixon, A.R., Walton, S.L., and Aridgides, L.J. The extracellular hyaluronidase gene (hylA) of Streptococcus pyogenes. FEMS Microbiol Lett **184,** 109, 2000.
10. Jiang, D., Liang, J., and Noble, P.W. Hyaluronan in tissue injury and repair. Annu Rev Cell Dev Biol **23,** 435, 2007.
11. Bitencourt, C.S., Pereira, P.A., Ramos, S.G., Sampaio, S.V., Arantes, E.C., Aronoff, D.M., and Faccioli, L.H. Hyaluronidase recruits mesenchymal-like cells to the lung and ameliorates fibrosis. Fibrogenesis Tissue Repair **4,** 3, 2011.
12. Girish, K.S., and Kemparaju, K. The magic glue hyaluronan and its eraser hyaluronidase: a biological overview. Life Sci **80,** 1921, 2007.
13. Mundargi, R.C., Babu, V.R., Rangaswamy, V., Patel, P., and Aminabhavi, T.M. Nano/micro technologies for delivering macromolecular therapeutics using poly(D,L-lactide-co-glycolide) and its derivatives. J Control Release **125,** 193, 2008.
14. Allen, T.M., and Cullis, P.R. Drug delivery systems: entering the mainstream. Science **303,** 1818, 2004.
15. Nicolete, R., Lima Kde, M., Júnior, J.M., Baruffi, M.D., de Medeiros, A.I., Bentley, M.V., Silva, C.L., and Faccioli, L.H. *In vitro* and *in vivo* activities of leukotriene B4-loaded biodegradable microspheres. Prostaglandins Other Lipid Mediat **83,** 121, 2007.
16. Wischke, C., and Schwendeman, S.P. Principles of encapsulating hydrophobic drugs in PLA/PLGA microparticles. Int J Pharm **364,** 298, 2008.
17. Dos Santos, D.F., Bitencourt, C.S., Gelfuso, G.M., Pereira, P.A., de Souza, P.R., Sorgi, C.A., Nicolete, R., and Faccioli, L.H. Biodegradable microspheres containing leukotriene B(4) and cell-free antigens from *Histoplasma capsulatum* activate murine bone marrow-derived macrophages. Eur J Pharm Sci **44,** 580, 2011.
18. dos Santos, D.F., Nicolete, R., de Souza, P.R., Bitencourt Cda, S., dos Santos, R.R., Jr., Bonato, V.L., Silva, C.L., and Faccioli, L.H. Characterization and *in vitro* activities of cell-free antigens from *Histoplasma capsulatum*-loaded biodegradable microspheres. Eur J Pharm Sci **38,** 548, 2009.
19. Shoyele, S.A. Engineering protein particles for pulmonary drug delivery. Methods Mol Biol **437,** 149, 2008.
20. Shoyele, S.A., and Cawthorne, S. Particle engineering techniques for inhaled biopharmaceuticals. Adv Drug Deliv Rev **58,** 1009, 2006.
21. Chow, A.H., Tong, H.H., Chattopadhyay, P., and Shekunov, B.Y. Particle engineering for pulmonary drug delivery. Pharm Res **24,** 411, 2007.
22. Bordon, K.C., Perino, M.G., Giglio, J.R., and Arantes, E.C. Isolation, enzymatic characterization and antiedematogenic activity of the first reported rattlesnake hyaluronidase from *Crotalus durissus terrificus* venom. Biochimie **94,** 2740, 2012.
23. Ortiz, L.A., Gambelli, F., McBride, C., Gaupp, D., Baddoo, M., Kaminski, N., and Phinney, D.G. Mesenchymal stem cell engraftment in lung is enhanced in response to bleomycin exposure and ameliorates its fibrotic effects. Proc Natl Acad Sci U S A **100,** 8407, 2003.
24. Hecker, L., Vittal, R., Jones, T., Jagirdar, R., Luckhardt, T.R., Horowitz, J.C., Pennathur, S., Martinez, F.J., and Thannickal, V.J. NADPH oxidase-4 mediates myofibroblast

activation and fibrogenic responses to lung injury. Nat Med **15,** 1077, 2009.
25. Padua, A.I., Silva, C.L., Ramos, S.G., Faccioli, L.H., and Martinez, J.A. Influence of a DNA-hsp65 vaccine on bleomycin-induced lung injury. J Bras Pneumol **34,** 891, 2008.
26. Tabata, Y., and Ikada, Y. Effect of the size and surface charge of polymer microspheres on their phagocytosis by macrophage. Biomaterials **9,** 356, 1988.
27. Champion, J.A., Walker, A., and Mitragotri, S. Role of particle size in phagocytosis of polymeric microspheres. Pharm Res **25,** 1815, 2008.
28. Lawrence, T., Willoughby, D.A., and Gilroy, D.W. Anti-inflammatory lipid mediators and insights into the resolution of inflammation. Nat Rev Immunol **2,** 787, 2002.
29. Dominici, M., Le Blanc, K., Mueller, I., Slaper-Cortenbach, I., Marini, F., Krause, D., Deans, R., Keating, A., Prockop, D.J., and Horwitz, E. Minimal criteria for defining multipotent mesenchymal stromal cells. The International Society for Cellular Therapy position statement. Cytotherapy **8,** 315, 2006.
30. Weiss, D.J., Bertoncello, I., Borok, Z., Kim, C., Panoskaltsis-Mortari, A., Reynolds, S., Rojas, M., Stripp, B., Warburton, D., and Prockop, D.J. Stem cells and cell therapies in lung biology and lung diseases. Proc Am Thorac Soc **8,** 223, 2011.
31. Wang, X., Hisha, H., Taketani, S., Adachi, Y., Li, Q., Cui, W., Cui, Y., Wang, J., Song, C., Mizokami, T., Okazaki, S., Li, Q., Fan, T., Fan, H., Lian, Z., Gershwin, M.E., and Ikehara, S. Characterization of mesenchymal stem cells isolated from mouse fetal bone marrow. Stem Cells **24,** 482, 2006.
32. Obayashi, Y., Yamadori, I., Fujita, J., Yoshinouchi, T., Ueda, N., and Takahara, J. The role of neutrophils in the pathogenesis of idiopathic pulmonary fibrosis. Chest **112,** 1338, 1997.
33. Kim, S.J., Angel, P., Lafyatis, R., Hattori, K., Kim, K.Y., Sporn, M.B., Karin, M., and Roberts, A.B. Autoinduction of transforming growth factor beta 1 is mediated by the AP-1 complex. Mol Cell Biol **10,** 1492, 1990.
34. de Figueiredo-Pontes, L.L., Assis, P.A., Santana-Lemos, B.A., Jácomo, R.H., Lima, A.S., Garcia, A.B., Thomé, C.H., Araújo, A.G., Panepucci, R.A., Zago, M.A., Nagler, A., Falcão, R.P., and Rego, E.M. Halofuginone has anti-proliferative effects in acute promyelocytic leukemia by modulating the transforming growth factor beta signaling pathway. PLoS One **6,** e26713, 2011.
35. Wang, Q., Wang, Y., Hyde, D.M., Gotwals, P.J., Koteliansky, V.E., Ryan, S.T., and Giri, S.N. Reduction of bleomycin induced lung fibrosis by transforming growth factor beta soluble receptor in hamsters. Thorax **54,** 805, 1999.
36. Grande, N.R., Peão, M.N.D., de Sá, C.M., and Águas, A.P. Lung fibrosis induced by bleomycin: structural changes and overview of recent advances. Scanning Microsc **12,** 487, 1998.
37. Siniscalco, D., Sullo, N., Maione, S., Rossi, F., and D'Agostino, B. Stem cell therapy: the great promise in lung disease. Ther Adv Respir Dis **2,** 173, 2008.
38. Moodley, Y., Atienza, D., Manuelpillai, U., Samuel, C.S., Tchongue, J., Ilancheran, S., Boyd, R., and Trounson, A. Human umbilical cord mesenchymal stem cells reduce fibrosis of bleomycin-induced lung injury. Am J Pathol **175,** 303, 2009.
39. Benjamin, D.K., Jr., Miller, W.C., Bayliff, S., Martel, L., Alexander, K.A., and Martin, P.L. Infections diagnosed in the first year after pediatric stem cell transplantation. Pediatr Infect Dis J **21,** 227, 2002.
40. Engelhard, D., Cordonnier, C., Shaw, P.J., Parkalli, T., Guenther, C., Martino, R., Dekker, A.W., Prentice, H.G., Gustavsson, A., Nurnberger, W., and Ljungman, P. Early and late invasive pneumococcal infection following stem cell transplantation: a European Bone Marrow Transplantation survey. Br J Haematol **117,** 444, 2002.
41. García-Castro, J., Trigueros, C., Madrenas, J., Pérez-Simón, J.A., Rodriguez, R., and Menendez, P. Mesenchymal stem cells and their use as cell replacement therapy and disease modelling tool. J Cell Mol Med **12**, 2552, 2008.

Address correspondence to:
Lúcia Helena Faccioli, PhD
Departamento de Análises Clínicas
Toxicológicas e Bromatológicas
Faculdade de Ciências Farmacêuticas de Ribeirão Preto
Universidade de São Paulo
Avenida do Café
S/N–Monte Alegre
Ribeirão Preto
SP 14040-903
Brazil

E-mail: faccioli@fcfrp.usp.br

Received: July 2, 2013
Accepted: July 15, 2014
Online Publication Date: December 23, 2014